

1 Article

## 2 **A comparison of U-net backbone architectures for the** 3 **automatic white blood cells segmentation**

4 **Mohammed Hakim BENDIABDALLAH** <sup>1,2\*</sup> and **Nesma SETTOUTI** <sup>2</sup>

5 <sup>1</sup> University of Ain Temouchent Belhadj Bouchaib, Ain-Temouchent, Algeria.

6 <sup>2</sup> Biomedical Engineering Laboratory, Faculty of Technology, University of Tlemcen, Algeria.

7 \* Correspondence: hakim.bendiabdallah@univ-tlemcen.dz

8 Received: date; Accepted: date; Published: date

9 **Abstract:** Reliable recognition of white blood cells is an essential step in the diagnosis of several  
10 types of cancer. Therefore, the segmentation of white blood cells plays an essential role and is an  
11 important part of the medical diagnostic system. Manual cell diagnosis involves doctors visually  
12 examining microscopic images to detect any cellular abnormalities. This step is costly and time-  
13 consuming. An automated system based on white blood cell identification provides a more accurate  
14 result than the manual method. Image segmentation is one of the crucial contributions of a deep  
15 learning community to the medical field. In this paper, we demonstrate how the U-Net type  
16 architecture can be improved by the use of the pre-trained encoder, a comparison of several efficient  
17 methods for automatic recognition of white blood cells using the original U-NET, different pre-  
18 trained classification networks are used as the backbone to obtain better performance. The  
19 architecture of RESNET-50 obtains the best segmentation results on testing data for automatic  
20 recognition in cytological images.

21 **Keywords:** white blood cells segmentation, deep Learning, transfer learning, U-NET, Loss Function,  
22 cytological image's dataset.  
23

---

### 24 1. Introduction

25 The expertise of spinal cord smears represents the cornerstone of hematological diagnosis.  
26 Indeed, the bone marrow is made up of stem cells from which blood cells (WBC) are produced, and  
27 in the event of an abnormality in one of the components of the blood (in the event of a deficiency or  
28 proliferation) the cells of the bone marrow can in be the cause. Unlike the blood smear, it is sufficient  
29 to focus on a microscopic field which seems adequate (many cells, well spread out and well stained)  
30 and to carry out the count of all the cells present in this field; then move to another field that seems  
31 adequate, and so on [1]. Clearly, this test is an important indicator in the detection of certain blood  
32 abnormalities. Blood morphology is made up of three elements: cells such as red blood cells  
33 (erythrocytes) and white blood cells (leukocytes) as well as blood platelets (not considered cells). The  
34 expression of the shape and number of white blood cells (WBC) has many quantitative and  
35 informative clues [2]. For example, increasing or decreasing white blood cells is very critical and may  
36 receive medical attention.

37 Within the framework of medical image analysis techniques, the segmentation of white blood  
38 cells is a key problem that we will refer to in this work. The segmentation of microscopic images uses  
39 information from the image (color, grayscale and spatial) to delineate different anatomical structures,  
40 including white blood cells (WBC) which are made up of nucleus and cytoplasm.

41 Several research works have been carried out on the semantic segmentation of blood stem cells  
42 from bone marrow [3–5]. In this work, we focus on citing the works and methods that have been  
43 proposed and applied to the real image of the cytological image's dataset [6] on which our study is

44 based. These microscopic images of blood stem cells of the bone marrow were collected within the  
45 Haemobiology Service, University Hospital Center of Tlemcen, Algeria, on slides staining type MGG  
46 (May Grunwald Giemsa).

47 Research works in the literature can be divided into four segmentation approaches:

48 *Morphological approaches:*

49 *Benazzouz et al.* [6] proposed an automated identification of plasma cells in bone marrow images.  
50 The steps of their segmentation model were divided into two phases. The first one used Otsu  
51 thresholding to extract the nucleus (green label) and the second one used the region growing on the  
52 obtained nucleus to delineate the cytoplasm. After segmentation, a classification of the obtained  
53 globules is used to count them. This method showed promising results when extracting the white  
54 blood cell named Leucocyte. Besides, segmentation of bone marrow images based on the Watershed  
55 transformation was proposed by *Baghli et al.* [7]. Its principle is to consider the image as a topographic  
56 map where the user must define starting points for the algorithm to flood the basins (objects to be  
57 detected) until there is a meeting point between the different basins (regions). Then the regions are  
58 merged by integrating the uncertainty on the color through the theory of evidence. In the end, the  
59 classification of the obtained globules is performed by three classifiers: SVM, Knn, and the decision  
60 tree. A Multi Features Based Approach for White Blood Cells Segmentation and Classification in  
61 Peripheral Blood and Bone Marrow Images was proposed by *Benomar et al.* [8]. It is a system that  
62 allows segmentation and differential counting of white blood cells, the process begins by highlighting  
63 WBCs by the stretch decorrelation method. Then, Otsu's thresholding is applied to the edited image  
64 using a color transformation. Segmentation is performed by Watershed to determine the boundaries  
65 of the blood cells followed by cleaning the image to remove false positives. At the end of this  
66 segmentation, a color scheme is used to separate the nucleus from the cytoplasm.

67 *Pixel-based Classification approaches:*

68 Pixel-based classification involves classifying each pixel in the image to a region class by  
69 machine learning approaches. Indeed, these methods perform a separation in the characteristic space  
70 of each pixel, the representation space can be constituted by the color or texture information so that  
71 a projection in this space achieves linear or non-linear boundaries between regions of the image. For  
72 white blood cell segmentation, *Settouti et al.* [9] proposed an automatic method based on region  
73 growth by classifying neighboring pixels from the pixels of interest in the image with minimal  
74 intervention by the expert. The points of interest are detected by the ultimate erosion morphological  
75 operator and two classifiers are applied for classification: Decision Tree (mono-classifier) and  
76 Random Forest (Multi-classifiers / ensemble method). We can say that the main limitation of this  
77 method is the long processing time, which makes it useless in a big data problem. In this case, two  
78 solutions have been proposed to resolve this problem, which is: Involving instance selection  
79 algorithms for a pixel reduction process that can reduce the cost of storing and computing image  
80 segmentation by selecting relevant pixels to the pixel-based classification task. *Saidi et al.* [10]  
81 proposed the EMIS Algorithm, an instance selection approach based on ensemble methods that use  
82 the ensemble margin as a selection criterion to overcome the problem of sensitivity to noise.  
83 Subsequently, in addition to this time saving, in another work, *Settouti et al.* [11] identify the relevant  
84 color spaces, which provide more information in the WBC segmentation process and eliminate the  
85 redundant and unnecessary characteristics of all images feature extraction. They proposed the IVsel  
86 algorithm "Instance & Variable selection", which highlights the importance of selecting only the most  
87 useful instances and variables to separate the different ROIs.

88 *Super-pixel-based Classification approaches:*

89 The current trend is towards the application of super-pixel classification which has great  
90 potential in the segmentation of color images in the segmentation process. It is a clustering technique  
91 that allows the image to be subdivided into  $k$  homogeneous clusters allowing to accelerate and

92 improve the quality of segmentation. *Bechar et al.* [12] developed a segmentation procedure based on  
93 super-pixel classification, where characterization based on image color information is done at the  
94 super-pixel level. They performed different ways of characterization to study the influence of color  
95 normalization, color information, and characterization technique on the segmentation results of  
96 white blood cells. The findings indicate that color normalization provides characterization precision  
97 and significant segmentation improvements. Besides, *Bechar et al.* [13] demonstrated the application  
98 potential of semi-supervision in the segmentation of cytological images and the recognition of white  
99 blood cells. A comparison is carried out between the multi-classifiers and the mono-classifier in  
100 supervised mode (random forests vs. Decision tree) and semi-supervised mode (co-Forest vs. Self-  
101 learning SETRED), the application of algorithms semi-supervised learning have shown their  
102 superiority over supervised learning.

103 *Deep Learning approaches:*

104 The advent of deep learning has eased the heavy lifting of the physician by making it possible  
105 to make accurate diagnoses in a short time. Particularly, Convolution Neuronal Networks (CNNs)  
106 have proven to be very robust in solving image classification problems and several architectures have  
107 been proposed to increase their performance, notably for microscopic images of the blood cells of the  
108 bone marrow. The success of deep learning methods in performing image classification has extended  
109 their use to solve more complex tasks including semantic segmentation by interpreting it as either a  
110 regression or discrimination problem. For the same case application of our work, recently, *Khouani et al.* [14]  
111 have conducted a study of deep learning methods for the automatic segmentation of regions  
112 of the nucleus and cytoplasm in cytological images. The proposed model is based on the use of Mask  
113 R-CNN with an improvement in the architecture and the stages of pre and post-processing. The  
114 results obtained are very promising and show the power of deep learning methods in the field of  
115 image processing.

116 In summary, as with the previously mentioned approaches, classical segmentation methods  
117 have major limitations that do not favor their deployment in clinics to perform critical tasks. If an  
118 approach is efficient, it requires a significant amount of execution time or human interaction. If the  
119 approach is automatic and does not require a learning mechanism, it is very sensitive to noise in the  
120 image. For methods requiring a learning mechanism, a detection phase is almost mandatory because  
121 the performance of the segmentation is closely linked to it. Moreover, the choice of the features to be  
122 extracted is problematic because even this restricts the scope of the method to a specific type of image  
123 where the classifier learns a feature of the structure to be segmented and not its global representation.  
124 This also limits the application of this type of method in the case where the anatomical structures are  
125 deformed. The success of deep learning (DL) lies mainly in its deference to traditional machine  
126 learning (ML) approaches. Indeed, ML models improve gradually but lack precision so the user must  
127 guide him by solving the problem explicitly, unlike DL which does it and can dispense with the  
128 feature extraction phase. Deep Learning has undergone a revolution over the past few years and an  
129 infinite number of architectures and models have been produced. Most of these models gave more  
130 than satisfactory results.

131 Through the literature review, we note that semantic segmentation of blood stem cells from bone  
132 marrow arouses a lot of interest within the scientific community. Classical approaches have provided  
133 initial solutions for WBC segmentation but with the shortcomings associated with each of the  
134 methods employed. Deep learning-oriented approaches have eliminated most of these limitations,  
135 but it nevertheless has several interrogations. First, the different architectures and models that exist  
136 make it difficult to choose the right network. Second, the hyperparameters of the network are difficult  
137 to evaluate a priori. Indeed, the number of layers, the number of neurons per layer, or the different  
138 connections between layers are crucial elements and essentially determined by a good intuition or by  
139 a succession of tests/calculation of errors (which is costly in time). The number of training samples is  
140 also a determining factor, and it often happens that this is too small compared to the number of  
141 parameters (weight) of the network. There are solutions such as artificially increasing their number  
142 or even reducing the number of free parameters (by pre-learning the first layers for example).

143 In this work, we have suggested a deep learning approach using U-Net to solve the problem of  
144 automatic recognition in cytological images, eight pre-trained encoder networks of U-Net models  
145 were appraised in the same experimental environment and with the same data. The distinction  
146 between white blood cells (leukocytes) in microscopic images of bone marrow and peripheral blood  
147 allows for accurate diagnoses of different cancers using a cost-effective method for fast, reliable, and  
148 efficient detection of nucleus and cytoplasm, which are clinically very important. We firstly exposed  
149 the most powerful structure for the encoder of U-Net in comparison to multiple deep learning  
150 models. Secondly, we have performed semantic segmentation with the best model, then we show the  
151 performance of the best model with examples. Finally, a comparison with other models is made.

152 The paper is organized as follows: materials and methods for the semantic segmentation of  
153 blood stem cells from bone marrow are presented in section 2. In section 3, we describe the cytological  
154 images dataset used in this study, with the experimental setting for the comparative study. In section  
155 4 experimental results are discussed. Finally, conclusions from this study and possible future works  
156 are presented in section 5.

## 157 2. Materials and Methods

158 There are several deep learning architectures that can solve this semantic segmentation problem.  
159 The general semantic segmentation network consists of an encoder and a decoder, U-Net  
160 architectures are normally considered as one of the most powerful tools for segmentation of  
161 biomedical images. We used different pre-trained CNN architectures as backbones of U-Net, and  
162 passing them to the U-Net decoder, we show how the performance of U-Net can be easily improved  
163 by using these backbones with pre-trained weights.

### 164 2.1. The model:

165 U-net [15] is an optimized semantic segmentation network based on Fully Convolutional  
166 Network (FCN). The architecture consists of a contracting path (encoder) to capture context and a  
167 symmetric expanding path (decoder) that enables precise localization and improves performance on  
168 segmentation tasks. We have chosen this model because the emergence of U-Net has brought great  
169 prospects for deep learning in the field of medical image analysis. It builds on previous convolutional  
170 networks to work more efficiently with fewer training images and to achieve more efficient  
171 segmentation. We used batch normalization before convolutional layers for internal covariate shift to  
172 achieve better performance and accelerate convergence [16]. Also, a dropout layer is utilized in the  
173 structure to reduce over-fitting problems.

### 174 2.2. Data augmentation

175 U-Net is capable of learning from a relatively small training set. In most cases, data sets for image  
176 segmentation consist of at most thousands of images, since manual preparation of the masks is a very  
177 costly procedure, so we used data augmentation. Data augmentation is essential to teach the network  
178 invariance and robustness properties. Using our small dataset of images and masks, we can generate  
179 new images that will be as insightful and useful to our model as our original images. Random  
180 transformations on the input images were used in the database augmentation. We randomly rotated  
181 inputs vertically and horizontally, then zoomed them. We also randomly increased and decreased  
182 the brightness of the images because the colour variation in the images was a significant segmentation  
183 complication due to the quality of the captor used during image capturing.

### 184 2.3 Transfer learning technique and training models:

185 Transfer learning is a popular approach in deep learning where pre-trained models are used as  
186 the starting point on computer vision processing tasks. It reduces training time considerably and  
187 leads to effective models [17,18] even with a small training set like ours.

188 We used the MobileNet [19], VGG [20], RESNET [21]) deep neural network as backbones (an  
189 encoder) in our U-Net network, the residual blocks in RESNET with skip connections helped in

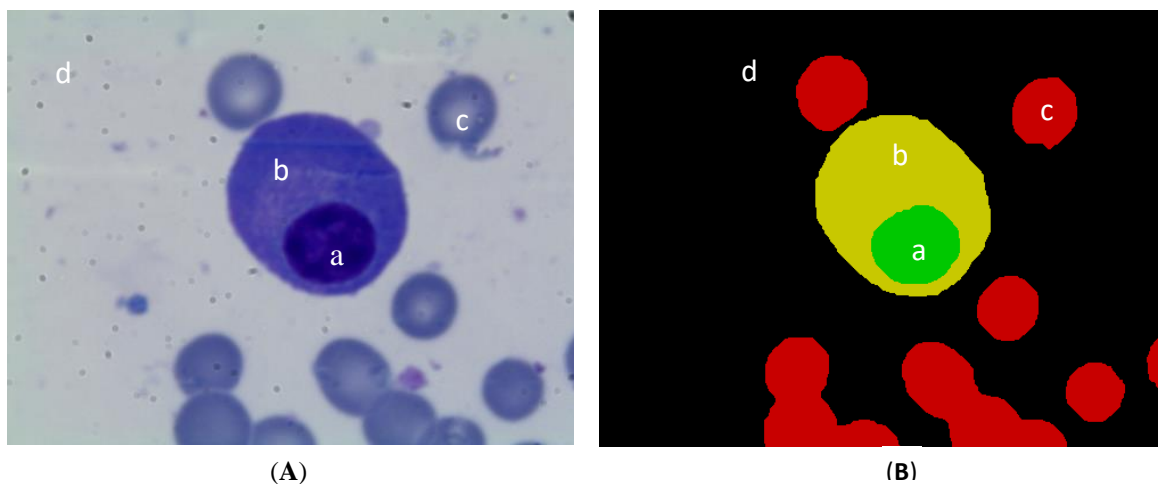
190 making a deeper and deeper convolution neural network and achieved record-breaking results for  
 191 classification on the ImageNet dataset. All mentioned backbones weights are pre-trained on The  
 192 ImageNet data set [22], the advantage of doing so is to shorten the learning procedure, which is done  
 193 by the last few layers of the network, to speed up convergence and to achieve high performance as  
 194 compared to a non-pre-trained model. We use these backbones as the first half (encoder) of U-net  
 195 [23]. Then, we train the decoder layers with our own augmented dataset. It helps save the training  
 196 procedure and enhances the advantage of U-net's ability to learn from small data.

197 During the convolutional neural network training, validation is used to detect when overfitting  
 198 starts, training is stopped when performance on the validation set starts to degrade in order to avoid  
 199 the overfitting on the training data ("early stopping") [24].

### 200 3. Results

#### 201 3.1. The cytological images dataset

202 The dataset belongs to the field of hematology. It contains microscopic images of the blood cells  
 203 of the bone marrow which were collected at the Haemobiology Service, University Hospital Center  
 204 of Tlemcen, Algeria by *Benazzouz et al.* [6]. This dataset contains 87 images acquired in the LEICA  
 205 environment (camera and microscope) in BMP format of size 1024x768 and magnification x100.  
 206 Figure 1 shows some images of this dataset in the top and their Ground Truth (bottom) where the  
 207 expert selects 4 regions: nucleus, cytoplasm, red blood cells and plasma.  
 208



209 **Figure 1.** Samples of cytological images dataset (A) with the ground truth (B), where: (a) Nucleus, (b)  
 210 cytoplasm, (c) red cell and (d) plasma.

211 The protocol for obtaining these images is known as the spinal cord smear (myelogram). It  
 212 consists of spreading bone marrow on a microscopic slide to be able to study the morphology of the  
 213 cells present as well as their number after being stained and fixed using the microscope. We have  
 214 chosen randomly 80% of the images for training and validation, then the rest for testing. For the  
 215 optimal configuration for our machine we have resized the images to 256x256

#### 216 3.2. Experimental setting

217 All experiments are performed on a computer with GeForce NVIDIA GTX 1060 graphics cards.  
 218 The proposed network models were implemented with python and TensorFlow v 2.2.0. We trained  
 219 our models using **Adam gradient-based optimization algorithm** with a learning rate of 1e-3, it is a  
 220 popular algorithm in the field of deep learning because is computationally efficient and has small  
 221 memory requirements [25].

222 We have determined the early stopping criterion at 10 training epochs both in the training and  
 223 validation phase for each architecture.

224 Loss function:

225 Since we can consider the image segmentation task as a pixel classification problem, the choice  
 226 of the loss function is very important while designing complex image segmentation. we used both  
 227 cross-entropy (CE) eq. (1) and Dice loss (DL) eq. (2) functions, then compared their performances to  
 228 find the best metric with our database.

229 Categorical Cross Entropy loss [26]:

$$CE(y, \hat{p}) = -(y \log(\hat{p}) + (1 - y) \log(1 - \hat{p})) \quad (1)$$

230 Here,  $\hat{p}$  is the predicted value by the prediction model and  $y$  is the ground truth.

231  
 232 Dice Loss [27]:

$$DL(y, \hat{p}) = 1 - \frac{2y\hat{p} + 1}{y + \hat{p} + 1} \quad (2)$$

233 Here, 1 is added in numerator and denominator to ensure that the function is not undefined in edge  
 234 case scenarios such as when  $y = \hat{p} = 0$ .

235  
 236 3.3. Evaluation Metrics

237 We have performed several experiments using data augmentation and Transfer learning for different  
 238 encoders pre-trained on ImageNet (MobileNet, MobileNet V2, RESNET 18, RESNET 34, RESNET 50,  
 239 RESNET 152, VGG 16, VGG 19), all images have a size of 256x256.

240 The classification performances are evaluated based on the Precision eq. (3) and the most used metrics  
 241 for semantic segmentation F1 Score (Dice Coefficient) eq. (4).

$$Precision = \frac{TP}{TP + FP} \quad (3)$$

$$F - score = Dice Coefficient = 2 * \frac{Precision \cdot Recall}{Precision + Recall} = 2 * \frac{TP}{2 * TP + FP + FN} \quad (4)$$

242 Where:

- 243 • True positives (TP): The intersection between segmentation and ground truth
- 244 • False positives (FP): Segmented parts not overlapping the ground truth
- 245 • False negatives (FN): Missed parts of the ground truth
- 246 • True negatives (TN): Part of the image beyond the union between segmentation and ground  
 247 truth.

248 **Table 1.** Performances, Epochs using Dice loss and Cross-entropy loss for each backbone.

Encoder	Metrics	Nucleus		Cytoplasm		Epochs	
		CrossEntr Loss	Dice Loss	CrossEntr Loss	Dice Loss	CrossEntr Loss	Dice Loss
U-NET	Precision	0,9798	0,9796	0,8853	0,8754	53	43
	F-score/Dice	0,9547	0,9496	0,9271	0,9192		
MOBILNET	Precision	0,9360	0,9863	0,8852	0,8639	14	23
	F-score/Dice	0,9434	0,9406	0,9152	0,9192		
MOBILENET V2	Precision	0,9936	0,9562	0,8600	0,8672	29	49
	F-score/Dice	0,9360	0,9450	0,9173	0,9123		
RESNET 50	Precision	0,9800	0,9900	0,8891	0,8816	13	37
	F-score/Dice	0,9577	0,9419	0,9314	0,9214		
VGG 19	Precision	0,9664	0,9806	0,8877	0,8703	38	52
	F-score/Dice	0,8154	0,9282	0,9206	0,9178		

<b>VGG 16</b>	<b>Precision</b>	0,9105	0,9701	0,8872	0,8554	27	69
	<b>F-score/Dice</b>	0,8707	0,9205	0,9010	0,9079		
<b>RESNET 152</b>	<b>Precision</b>	0,9440	0,9878	0,8934	0,8720	24	44
	<b>F-score/Dice</b>	0,9477	0,9400	0,9226	0,9231		
<b>RESNET 34</b>	<b>Precision</b>	0,9754	0,9878	0,8803	0,8814	16	41
	<b>F-score/Dice</b>	0,9485	0,9493	0,9252	0,9284		
<b>RESNET 18</b>	<b>Precision</b>	0,9202	0,9807	0,8921	0,8871	22	36
	<b>F-score/Dice</b>	0,9269	0,9435	0,9111	0,9284		

**Bold numbers** represent the best results using F-Score

249 **4. Discussion**

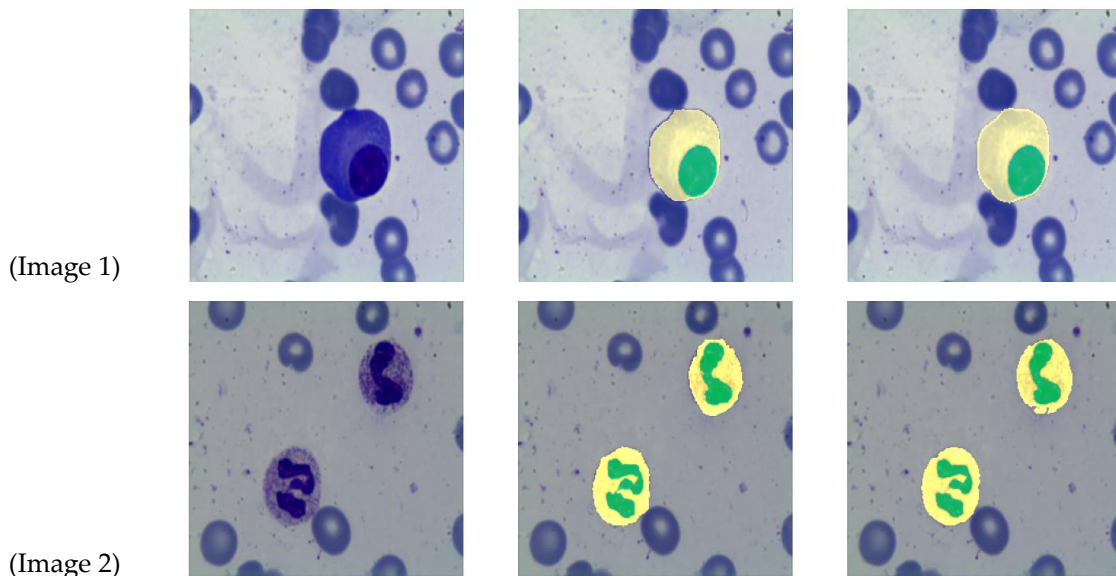
250 Results in Table 1 demonstrated that the use of Standard U-Net and RESNET-50 gives the best  
 251 performance, but RESNET-50 converges to better results in only 13 epochs using the Cross-entropy  
 252 loss function, Dice score has achieved a promising result for nucleus and cytoplasm segmentation:  
 253 **0,957** and **0,931** respectively. We remind that we have determined the early stopping criterion at 10  
 254 training epochs for each architecture if the loss function does not improve after 10 iterations, because  
 255 too many epochs can lead to overfitting of the training dataset.

256 **Table 2.** Performances, using Dice loss and Cross-entropy loss for RESNET-50 encoder.

	<b>Nucleus</b>		<b>Cytoplasm</b>	
	<b>CrossEntr Loss</b>	<b>Dice Loss</b>	<b>CrossEntr Loss</b>	<b>Dice Loss</b>
<b>Precision</b>	<b>0.9800</b>	<b>0.9900</b>	<b>0.8891</b>	0.8816
<b>Sensitivity</b>	<b>0.9365</b>	<b>0.8982</b>	<b>0.9780</b>	0.9651
<b>Specificity</b>	<b>0.9994</b>	<b>0.9997</b>	<b>0.9942</b>	0.9938
<b>F-Score/Dice</b>	<b>0.9577</b>	<b>0.9419</b>	<b>0.9314</b>	0.9214
<b>IoU/Jaccard</b>	<b>0.9189</b>	<b>0.8902</b>	<b>0.8717</b>	0.8543

257 The specificity using RESNET-50 pre-trained encoder is practically equal to 1, this means the  
 258 system avoid false alarms, the clinician is more assured in the automatic system.

259





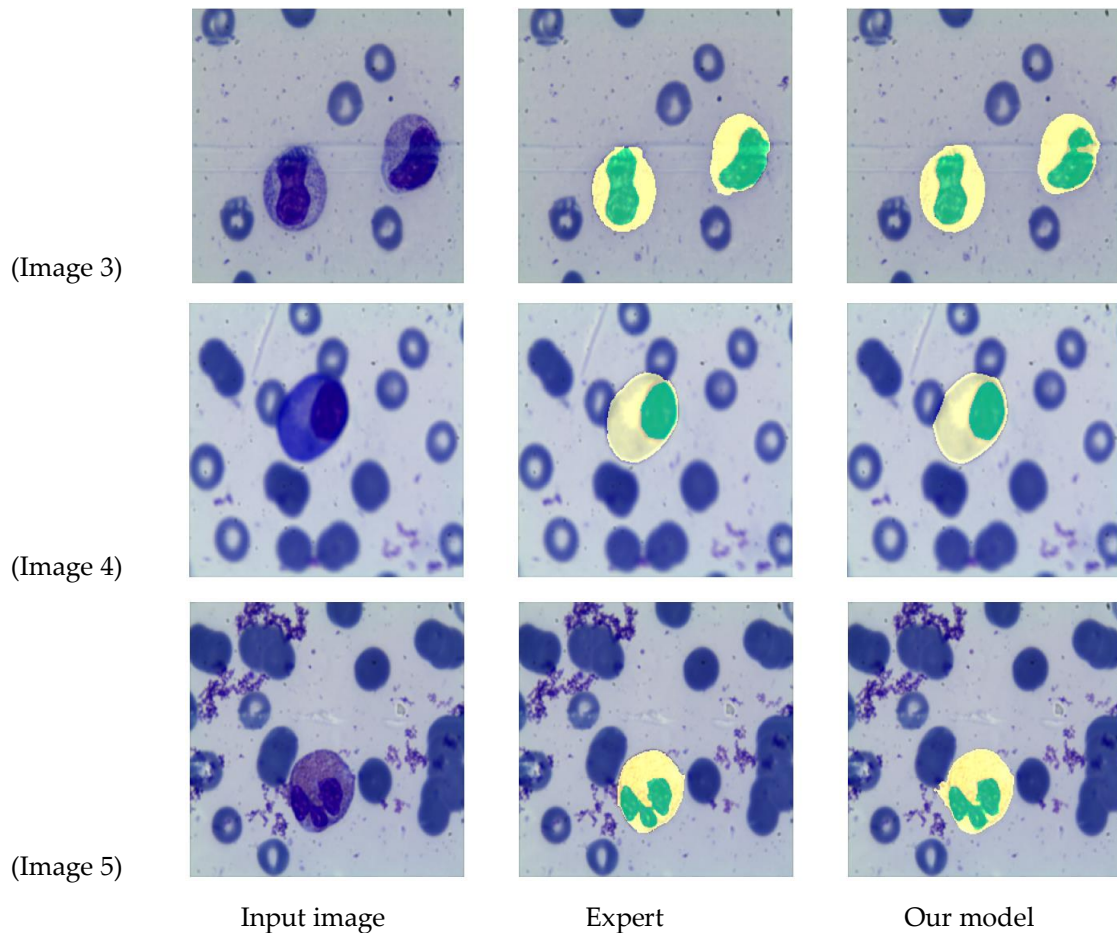


**Figure 2.** Results of automatic segmentation by U-NET using RESNET-50 Encoder

260

261 We randomly select five images from the test database (Figure 2) to discuss the performance of  
 262 our semantic segmentation model. We overlapped the mask on the original image to have better  
 263 visibility of the segmentation quality. We note that the separation of cytoplasm and nuclei is almost  
 264 identical to the expert's labeling, also the model can distinguish white blood cells from red blood  
 265 cells, for example in Image 4 (Figure 2).

266 We find that the color variation in the images does not affect the segmentation, this is partly due  
 267 to data augmentation and to be precise, the fact of increasing and decreasing the brightness.

268 These results can affirm the effectiveness and great speed of response compared to other  
 269 methods (small number of epochs) using transfer learning (with pre-trained weights on ImageNet).  
 270 The use of RESNET-50 as backbone gives the best results, we can explain this by using a deeper  
 271 convolution network through series of residual blocks (with skip connections) to help us address  
 272 the vanishing gradient problem.

273 Having demonstrated the superiority of the RESNET-50 as a backbone model over other models,  
 274 in Table 3, we will now briefly compare the results we obtained in this study with those of previous  
 275 works.

276

**Table 3.** Comparison with related works on WBC segmentation method with the same dataset.

Authors	Model/Algorithm	Nucleus		Cytoplasm	
		Precision	F-Score/Dice	Precision	F-Score/Dice
Benazzouz et al. [6]	Otsu + classification	95.02	-	84.53	-
Baghli et al. [7]	Evidence theory	95.90	-	88.4	-
Benomar et al. [8]	Otsu + watershed	96.87	-	92.50	-
Settouti et al. [9]	Pixel-based approach	<b>99.12</b>	0.9532	<b>97.15</b>	0.8982



Saidi et al. [10]	EMIS	99.05	0.88	95.05	0.61
Settouti et al. [11]	IVsel	99.10	0.84	94.99	0.4518
Our Approach	U-Net RESNET-50	98.00	<b>0.9577</b>	88.91	<b>0.9314</b>

277

278

If we compare the performances of the quoted works in Table 3, we can establish the following remarks:

279

280

- The previous results of *Settouti et al.* [9] for nucleus recognition were better than ours, but our approach gave the best results according to the Dice coefficient for nucleus and cytoplasm segmentation which demonstrates that our model has a higher sensitivity in detecting the relevant objects.

281

282

283

284

- Furthermore, the use of the U-Net architecture combined with the pre-trained RESNET-50 encoder allowed for fast learning and segmentation. In contrast to the limitations of other traditional methods that require long processing times [9].

285

286

287

## 5. Conclusions

288

This paper reports important results achieved using different models for the encoder part of the U-Net for the automatic recognition of nuclei and cytoplasm regions in cytological images to help experts in medical diagnosis, sometimes even an expert might make a mistake in this so automating the full pipeline. The objective is to automatically detect each object in the image and classify it as a nucleus or a cytoplasm while forming a binary mask to perform the segmentation. Our results were very promising and encouraging, especially by using pre-trained RESNET-50 as the backbone with the loss function adapted to our task, it helped us to address the vanishing gradient problem, increasing the segmentation quality and speed.

289

290

291

292

293

294

295

296

However, there are further developments in future works to improve the model that performs cell instance segmentation, to distinguish adjacent cells, and to identify individual cells.

297

298

**Funding:** This research received no external funding.

299

**Acknowledgments:** The authors would like to thank the Directorate-General of Scientific Research and Technological Development (Direction Générale de la Recherche Scientifique et du Développement Technologique, DGRSDT, URL: [www.dgrsdt.dz](http://www.dgrsdt.dz), Algeria) for the financial assistance towards this research.

300

301

302

**Conflicts of Interest:** The authors declare no conflict of interest.

303

## References

304

1. Al-Dulaimi, K.A.K.; Banks, J.; Chandran, V.; Tomeo-Reyes, I.; Thanh, K.N. Classification of white blood cell types from microscope images: Techniques and challenges. In *Microscopy science: Last approaches on educational programs and applied research (Microscopy Book Series, 8)*; Mendez-Vilas, A., Torres-Hergueta, E., Eds.; Formatex Research Center: Spain, 2018; pp. 17–25.

305

306

307

308

2. Blumenreich, M.S. The White Blood Cell and Differential Count. BTI - Clinical Methods: The History, Physical, and Laboratory Examinations. In: H Kenneth Walker W Dallas Hall, J.W.H., Ed.; Butterworths: Emory University School of Medicine, Atlanta, Georgia FAU - Blumenreich, Martin S, 1990.

309

310

311

3. Yu, T.-C.; Chou, W.-C.; Yeh, C.-Y.; Yang, C.-K.; Huang, S.-C.; Tien, F.M.; Yao, C.-Y.; Cheng, C.-L.; Chuang, M.-K.; Tien, H.-F.; et al. Automatic Bone Marrow Cell Identification and Classification By Deep Neural Network. *Blood* 2019, 134, 2084, doi:10.1182/blood-2019-125322.

312

313

314

4. Ramakrishna, R.R.; Abd Hamid, Z.; Zaki, W.M.D.W.; Huddin, A.B.; Mathialagan, R. Stem cell imaging through convolutional neural networks: current issues and future directions in artificial intelligence technology. *PeerJ* 2020, 8, e10346.

315

316

317

5. Anilkumar, K.K.; Manoj, V.J.; Sagi, T.M. A survey on image segmentation of blood and bone marrow smear images with emphasis to automated detection of Leukemia. *Biocybern. Biomed. Eng.* 2020, 40, pp. 1406–1420, doi:https://doi.org/10.1016/j.bbe.2020.08.010.

318

319

320

6. Benazzouz, M.; Baghli, I.; Chikh, M.A. Microscopic image segmentation based on pixel classification and dimensionality reduction. *Int. J. Imaging Systems and Technology* 2013, 23, pp. 22–28.

321

322

323

7. Baghli, I.; Nakib, A.; Sellam, E.; Benazzouz, M.; Chikh, A.; Petit, E. Hybrid framework based on evidence theory for blood cell image segmentation. *Medical Imaging 2014: Biomedical Applications in Molecular,*

- 324 Structural, and Functional Imaging; Molthen, R.C.; Weaver, J.B., Eds. International Society for Optics and  
325 Photonics, SPIE, **2014**, Vol. 9038, pp. 314 – 321. doi:black10.1117/12.2042142.
- 326 8. Benomar, M.L.; Chikh, A.; Descombes, X.; Benazzouz, M. Multi-feature-based approach for white blood  
327 cells segmentation and classification in peripheral blood and bone marrow images. *International Journal of*  
328 *Biomedical Engineering and Technology* **2021**, 35, pp. 223–241.
- 329 9. Settouti, N.; Bechar, M.E.A.; El Habib Daho, M.; Chikh, M.A. An optimised pixel-based classification  
330 approach for automatic white blood cells segmentation. *International Journal of Biomedical Engineering and*  
331 *Technology* **2020**, 32, pp. 144–160.
- 332 10. Saidi, M.; Bechar, M.E.A.; Settouti, N.; Chikh, M.A. Instances selection algorithm by ensemble margin.  
333 *Journal of Experimental & Theoretical Artificial Intelligence* **2018**, 30, pp. 457–478,  
334 doi:black10.1080/0952813X.2017.1409283.
- 335 11. Settouti, N.; Saidi, M.; Bechar, M.E.A.; El Habib Daho, M.; Chikh, M.A. An instance and variable selection  
336 approach in pixel-based classification for automatic white blood cells segmentation. *Pattern Analysis and*  
337 *Applications* **2020**, 23, pp. 1709–1726.
- 338 12. Bechar, M.E.A.; Settouti, N.; Daho, M.E.H.; Adel, M.; Chikh, M.A. Influence of normalization and color  
339 features on super-pixel classification: application to cytological image segmentation. *Australasian Physical*  
340 *& Engineering Sciences in Medicine* **2019**, 42, pp. 427–441.
- 341 13. Bechar, M.E.A.; Settouti, N.; Daho, M.E.H. Semi-supervised Super-pixels classification for White Blood  
342 Cells segmentation. 2018 3rd International Conference on Pattern Analysis and Intelligent Systems (PAIS),  
343 **2018**, pp. 1–8. doi:black10.1109/PAIS.2018.8598521.
- 344 14. Khouani, A.; El Habib Daho, M.; Mahmoudi, S.A.; Chikh, M.A.; Benzineb, B. Automated recognition of  
345 white blood cells using deep learning. *Biomedical Engineering Letters* **2020**, 10, pp. 359–367.
- 346 15. Ronneberger, O.; Fischer, P.; Brox, T. U-net: Convolutional networks for biomedical image segmentation.  
347 International Conference on Medical image computing and computer-assisted intervention. Springer, **2015**,  
348 pp. 234–241.
- 349 16. Ioffe, S.; Szegedy, C. Batch normalization: accelerating deep network training by reducing internal  
350 covariate shift. *arXiv e-prints* **2015**.
- 351 17. Igloukov, V.; Shvets, A. Ternaunet: U-net with vgg11 encoder pre-trained on imagenet for image  
352 segmentation. *arXiv preprint arXiv:1801.05746* **2018**.
- 353 18. Chang, S.W.; Liao, S.W. KUNet: microscopy image segmentation with deep unet based convolutional  
354 networks. 2019 IEEE International Conference on Systems, Man and Cybernetics (SMC). IEEE, **2019**, pp.  
355 3561–3566.
- 356 19. Howard, A.G.; Zhu, M.; Chen, B.; Kalenichenko, D.; Wang, W.; Weyand, T.; Andreetto, M.; Adam, H.  
357 Mobilenets: Efficient convolutional neural networks for mobile vision applications. *arXiv preprint*  
358 *arXiv:1704.04861* **2017**.
- 359 20. Simonyan, K.; Zisserman, A. Very deep convolutional networks for large-scale image recognition. *arXiv*  
360 *preprint arXiv:1409.1556* **2014**.
- 361 21. He, K.; Zhang, X.; Ren, S.; Sun, J. Deep residual learning for image recognition. Proceedings of the IEEE  
362 conference on computer vision and pattern recognition, **2016**, pp. 770–778.
- 363 22. Russakovsky, O.; Deng, J.; Su, H.; Krause, J.; Satheesh, S.; Ma, S.; Huang, Z.; Karpathy, A.; Khosla, A.;  
364 Bernstein, M.; others. Imagenet large scale visual recognition challenge. *International journal of computer*  
365 *vision* **2015**, 115, pp. 211–252.
- 366 23. Yakubovskiy, P. Segmentation Models. [https://github.com/qubvel/segmentation\\_models](https://github.com/qubvel/segmentation_models), **2019**.
- 367 24. Prechelt, L. Early stopping-but when? In *Neural Networks: Tricks of the trade*; Springer, **1998**; pp. 55–69.
- 368 25. Kingma, D.P.; Ba, J. Adam: A method for stochastic optimization. *arXiv preprint arXiv:1412.6980* **2014**.
- 369 26. Yi-de, M.; Qing, L.; Zhi-Bai, Q. Automated image segmentation using improved PCNN model based on  
370 cross-entropy. Proceedings of 2004 International Symposium on Intelligent Multimedia, Video and Speech  
371 Processing, 2004. IEEE, **2004**, pp. 743–746.
- 372 27. Sudre, C.H.; Li, W.; Vercauteren, T.; Ourselin, S.; Cardoso, M.J. Generalised dice overlap as a deep learning  
373 loss function for highly unbalanced segmentations. In *Deep learning in medical image analysis and*  
374 *multimodal learning for clinical decision support*; Springer, **2017**; pp. 240–248.